

Polyfunctional Tetraaza-Macrocyclic Ligands: Zn(II), Cu(II) Binding and Formation of Hybrid Materials with Multiwalled Carbon Nanotubes

Matteo Savastano,[†] Paloma Arranz-Mascarós,[‡] Carla Bazzicalupi,[†] Maria Paz Clares,[§] Maria Luz Godino-Salido,[‡] Lluís Guíjarro,[§] Maria Dolores Gutiérrez-Valero,[‡] Antonio Bianchi,^{*,†,‡} Enrique García-España,^{*,§} and Rafael López-Garzón^{*,‡}

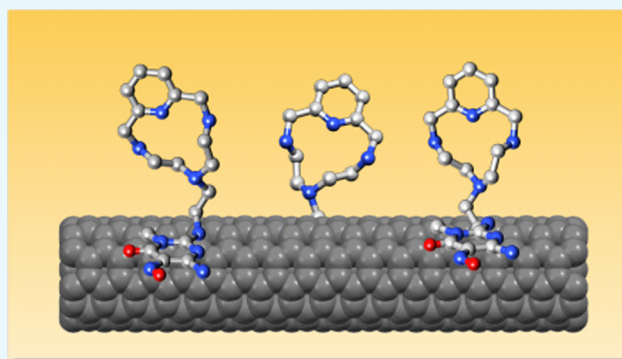
[†]Department of Chemistry "Ugo Schiff", University of Florence, 50019 Sesto Fiorentino, Italy

[‡]Department of Inorganic and Organic Chemistry, University of Jaén, 23071 Jaén, Spain

[§]Institute of Molecular Science, University of Valencia, 46071 Valencia, Spain

S Supporting Information

ABSTRACT: The binding properties of HL1, HL2, and HL3 ligands toward Cu(II) and Zn(II) ions, constituted by tetraaza-macrocyclic rings decorated with pyrimidine pendants, were investigated by means of potentiometric and UV spectrophotometric measurements in aqueous solution, with the objective of using the related HL-M(II) (HL = HL1–HL3; M = Cu, Zn) complexes for the preparation of hybrid MWCNT-HL-M(II) materials based on multiwalled carbon nanotubes (MWCNTs), through an environmentally friendly noncovalent procedure. As shown by the crystal structure of [Cu(HL1)](ClO₄)₂, metal coordination takes place in the macrocyclic ring, whereas the pyrimidine residue remains available for attachment onto the surface of the MWCNTs via π – π stacking interactions. On the basis of equilibrium data showing the formation of highly stable Cu(II) complexes, the MWCNT-HL1-Cu(II) material was prepared and characterized. This compound proved very stable toward lixiviation processes (release of HL1 and/or Cu(II)); thus, it was used for the preparation of its reduced MWCNT-HL1-Cu(0) derivatives. X-ray photoelectron spectroscopy and transmission electron microscopy images showed that MWCNT-HL1-Cu(0) contains Cu(0) nanoparticles, of very small (less than 5 nm) and regular size, uniformly distributed over the surface of the MWCNTs. Also, the MWCNT-HL1-Cu(0) material proved very resistant to detachment of its components. Accordingly, both MWCNT-HL1-Cu(II) and MWCNT-HL1-Cu(0) are promising candidates for applications in heterogeneous catalysis.



INTRODUCTION

In a recent work, we performed the synthesis of HL1 and HL2 ligands obtained via functionalization of the tetraaza-macrocyclic molecules **1** and **2** with a 6-amino-3,4-dihydro-3-methyl-5-nitroso-4-oxypyrimidine group (Figure 1).¹ Thanks to the ability of such pyrimidine residues to form strong π – π stacking interactions with arene centers,² HL1 and HL2 were irreversibly absorbed onto the surface of multiwalled carbon nanotubes (MWCNTs) and the resulting hybrid materials (MWCNT-HL1, MWCNT-HL2) were further decorated with Pd(II) ions coordinated to the macrocyclic rings. The final products (MWCNT-HL1-Pd, MWCNT-HL2-Pd) were assayed as heterogeneous catalysts for the Cu-free Sonogashira coupling reaction, in which respect they revealed high efficiency, ranking among the best Pd(II)-based heterogeneous catalysts in terms of yields and reaction times, and an unprecedented ability to work under environmentally friendly conditions, such as in water at 50 °C and in an aerobic

atmosphere.¹ Macrocyclic ligands were chosen to retain Pd(II) on the surface of MWCNTs because they form complexes with high thermodynamic stability and high kinetic inertness toward demetallation processes, characteristics that contribute to the robustness of the catalysts and favor their reusability.

In addition to their efficiency as active centers in many catalytic processes, metal ions fixed into the frames of macrocyclic ligands have proven useful for a variety of applications, including the construction of large self-assembled structures, molecular sensors, switches, motors, and machines; for mimicking biological processes; and for tissue and organ imaging, among others.³ For this reason, and in consideration of the successful results given by the Pd(II)-based heterogeneous catalysts with HL1 and HL2, we decided to assay the

Received: June 6, 2017

Accepted: July 7, 2017

Published: July 25, 2017

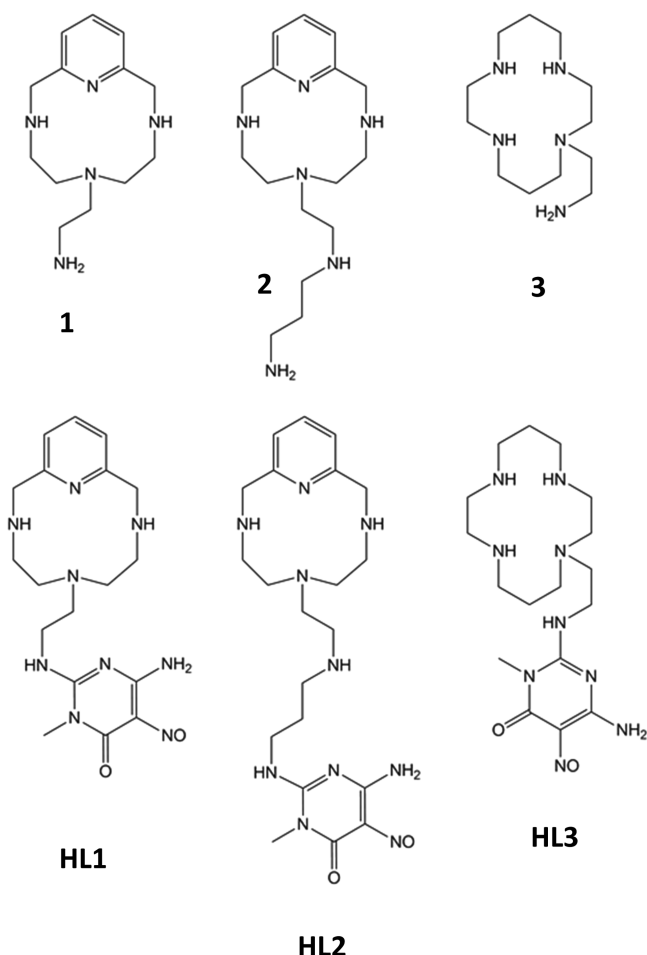


Figure 1. HL1, HL2, and HL3 ligands with their precursor molecules 1, 2, and 3.

binding ability of HL1 and HL2 toward other metal ions, and Zn(II) and Cu(II) were chosen, in view of their possible applications and on account of their implication as catalysts in a variety of reactions.^{4–6} In this respect, the ability of a hybrid material of the MWCNT-HL1 type to adsorb Cu(II) and Zn(II) metal ions from aqueous solution was also tested. For the same purpose, we synthesized the analogous ligand HL3

(Figure 1), containing cyclam (1,4,8,11-tetraazacyclotridecane), the most typical tetraaza-macrocyclic molecule, and extended to this new ligand the coordination study with Zn(II) and Cu(II). Among tetraaza-macrocycles, cyclam is the one able to form metal complexes with utmost stability with many metal ions.⁷ A potential catalyst based on Cu(0)-supported nanoparticles was generated from MWCNT-HL1-Cu(II).

RESULTS AND DISCUSSION

Crystal Structure of [Cu(HL1)](ClO₄)₂. The crystal structure consists of a one-dimensional (1D) coordination polymer, {[CuHL1]²⁺}_n, built up by repeats of complex units. A segment of the 1D polymer is shown in Figure 2, evidencing the metal coordination sphere (selected bond angles and distances are listed in Table 1).

Table 1. Selected Bond Angles (deg) and Distances (Å) for the Crystal Structure of [Cu(HL1)](ClO₄)₂^a

Cu–N4	2.068(5)
Cu–N1	2.324(5)
Cu–N3	1.933(5)
Cu–N2	2.060(6)
Cu–N8	2.003(5)
Cu–O1	2.534(4)
N4–Cu–N1	82.7(2)
N4–Cu–N3	82.3(2)
N4–Cu–N2	157.6(2)
N4–Cu–N8	107.6(2)
N4–Cu–O1	81.5(2)
N1–Cu–N3	97.4(2)
N1–Cu–N2	84.0(2)
N1–Cu–N8	108.4(2)
N1–Cu–O1	163.6(2)
N3–Cu–N2	81.7(2)
N3–Cu–N8	153.2(2)
N3–Cu–O1	84.9(2)
N2–Cu–N8	93.6(2)
N2–Cu–O1	112.4(2)
N8–Cu–O1	72.4(2)

^aSymmetry relation for N8 and O1 atoms: 1 – x, y – 0.5, 1.5 – z; e.s.d. in parentheses.

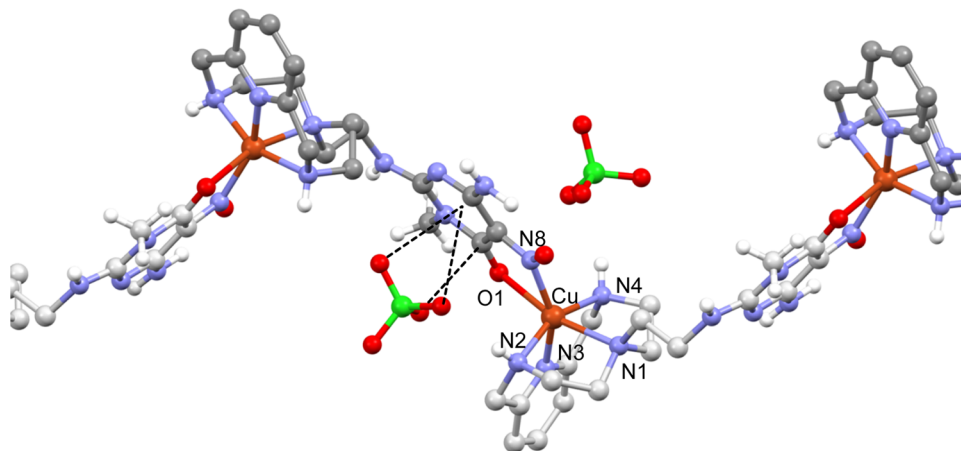


Figure 2. Segment of the 1D polymer in the crystal structure of CuHL1(ClO₄)₂ showing the metal coordination environment and the anion–π interaction of a perchlorate anion with the pyrimidine function of the ligand.

The copper atom is hexacoordinated by the four nitrogen atoms of the macrocycle and by the carbonyl oxygen and nitroso nitrogen belonging to the nitroso-amino pyrimidine group of a contiguous, symmetry-related ligand. The coordination sphere can be best described as a strongly distorted octahedron, whose axial distances, defined by the nitroso oxygen (O1) and the macrocyclic tertiary nitrogen (N1), are strongly elongated (Table 1). The equatorial plane is defined by the pyridine and the two secondary nitrogen atoms of the macrocycle, together with the nitroso nitrogen from the pyrimidine ring of the contiguous symmetry-related ligand. It is to be underlined that although the coordination of the nitroso nitrogen clearly acts on the electron distribution in the pyrimidine ring system, giving a remarkable shortening of the N=O bond and a lengthening of the N–C bond, the coordination of the carbonyl oxygen does not determine the weakening of the C=O bond, which is even shorter than the corresponding mean bond length of free C=O (1.205(7) Å vs 1.22(2) Å for C=O and 1.26(3) Å for C=O–M bonds). The head-to-tail disposition of the ligands in the chain is due to the 2_1 screw axes, running parallel to the b axis and determining an overall helical fashion for the coordination polymer.

Similarly to the crystal structures previously reported for metal complexes obtained with the 3,6,9-triaza-1-(2,6)-pyridinecyclodecaphane macrocycle functionalized on its 6 position,⁸ the macrocycle adopts a bent conformation, which leaves the metal coordination sphere unsaturated. In these structures, however, the macrocycle and the pendant arm containing donor atoms are involved in the coordination of the same metal center and isolated complexes are invariably formed. Instead, in the $\{[\text{CuHL1}]^{2+}\}_n$ polymer, the pendant arm and the macrocycle do not coordinate with the same metal ion so that the pyrimidine ring protrudes outside, and the metal coordination positions not saturated by the macrocycle are occupied by exogenous species.

Electroneutrality is achieved by the presence of two perchlorate anions in the asymmetric unit. One of them strongly interacts with the nitroso pyrimidine group via anion– π interactions with three out of four oxygen atoms (Table S1). Remarkably, one of the strongest anion– π interactions ever observed was reported for a ligand (L) containing this nitroso-amino pyrimidine group functionalized with a tren (tris(2-aminoethyl)amine) moiety. In the crystal structure of the $\{\text{H}_4\text{L}[\text{Co}(\text{CN})_6]\cdot 2\text{H}_2\text{O}\}$ compound, the nitrogen atom of a cyanide ion of $[\text{Co}(\text{CN})_6]^{3-}$ was found 2.786 Å apart from the ring centroid.⁹ In this structure, as well as in those obtained for the same ligand with HgCl_4^{2-} , HgBr_4^{2-} , and CdI_4^{2-} , the anions are pretty well localized above the ring centroid,⁹ whereas in $[\text{Cu}(\text{HL1})(\text{ClO}_4)_2]$, the ClO_4^- -pyrimidine interaction appears dominated by the contact of one perchlorate oxygen with the carbonyl C atom of the pyrimidine ring. The O11...C17 contact distance (2.872(8) Å) is almost coincident with the O...ring plane distance (2.882 Å). The O13 and O14 oxygen atoms are 3.238 and 3.813 Å apart from the ring centroid and can be considered localized on the ring periphery, having offsets of 0.81 and 2.13 Å, respectively.

Acid–Base Properties of HL3. Potentiometric (pH-metric) titrations performed in aqueous solution (0.1 M Me_4NCl , 298.1 K) in the pH range of 2.5–11.5 showed that HL3 contains four groups undergoing protonation and an acidic group that starts being deprotonated above pH 10. Table 2 lists the equilibrium constants determined for these processes in the form of protonation constants.

Table 2. Protonation Constants of Ligands HL1, HL2, and HL3 (L) in 0.1 M NMe_4Cl at 298.1 ± 0.1 K

equilibria	log K		
	HL1 ^a	HL2 ^a	HL3
$\text{L}^- + \text{H}^+ = \text{HL}$	11.13(4) ^b	11.21(5)	11.22(3)
$\text{HL} + \text{H}^+ = \text{H}_2\text{L}^+$	9.28(5)	9.71(4)	10.43(3)
$\text{H}_2\text{L}^+ + \text{H}^+ = \text{H}_3\text{L}^{2+}$	7.83(7)	8.64(6)	8.55(4)
$\text{H}_3\text{L}^{2+} + \text{H}^+ = \text{H}_4\text{L}^{3+}$	2.3(1)	7.51(6)	3.23(5)
$\text{H}_4\text{L}^{3+} + \text{H}^+ = \text{H}_5\text{L}^{4+}$	1.6(5)	2.2(1)	1.99(5)
$\text{H}_5\text{L}^{4+} + \text{H}^+ = \text{H}_6\text{L}^{5+}$		1.6(5)	

^aTaken from ref 1. ^bValues in parentheses are standard deviations of the last significant figures.

For the sake of comparison, the table includes the protonation constants previously determined for HL1 and HL2. A distribution diagram of the protonated species formed as a function of pH is reported in Figure S1. The protonation behavior of HL3 is consistent with that of HL1 and HL2, in particular with that of HL1, which is structurally more similar to HL3 (Figure 1). Accordingly, the protonation stage occurring at the highest pH (log K = 11.22, Table 2) can be ascribed to the nitrogen atom of the chain directly connected to the pyrimidine ring, which is expected to be deprotonated at a high pH, whereas protonation occurring at the lowest pH (log K = 1.99, Table 2) involves the pyrimidine nitroso group. This behavior is confirmed by the pH dependence of the absorption spectra of HL3. Indeed, the near-UV spectra of HL3 are characterized by three bands centered at about 328, 276, and 230 nm (Figure 3) corresponding to allowed π – π^* transitions between the π -orbitals of the pyrimidinic group and overlapping with the band at about 265 nm of the pyridinic one. The spectra show a significant pH dependence in acidic and alkaline solutions when protonation involves the pyrimidine chromophore, whereas they are almost invariant in the pH region 4.6–10 when protonation takes place on the non-chromogenic aliphatic amine groups. Very similar spectral features were found for HL1 and HL2.¹

The highly protonated H_5L^{4+} species is formed only in small amounts in the lower-pH region we have investigated (Figure S1). Nevertheless, the detection of this species is an important result revealing that, as previously observed for HL1 and HL2 as well as for HL3, three out of the four nitrogen atoms of the macrocyclic ring can undergo protonation in the studied pH range.

Formation of Metal Complexes in Solution. The equilibrium constants for the formation of Zn(II) and Cu(II) complexes with HL1, HL2, and HL3, determined in aqueous solution (0.1 M Me_4NCl , 298.1 K) by means of potentiometric (pH-metric) titrations, are listed in Table 3. In the case of the Cu(II) complexes with HL3, because of the slowness of both complexation and dissociation reactions, we were able to study the system in a restricted pH range (2.5–8) and after special manipulation of the samples (see Experimental Section). For this reason, larger errors were obtained for the determined stability constants. Distribution diagrams for the formation of these complexes are presented in Figure S2. In terms of the species formed, the three ligands (HL = HL1, HL2, HL3) give rise to identical complex systems with Zn(II), constituted by ZnL^+ , ZnHL^{2+} , $\text{ZnH}_2\text{L}^{3+}$, and ZnLOH species, whereas in the case of Cu(II), there are some differences. In particular, HL1 forms CuL^+ , CuHL^{2+} , $\text{CuH}_2\text{L}^{3+}$, and CuL^{5+} , whereas HL2 forms CuL^{2+} , CuHL^{2+} , $\text{CuH}_2\text{L}^{3+}$, and $\text{CuH}_3\text{L}^{6+}$. HL3

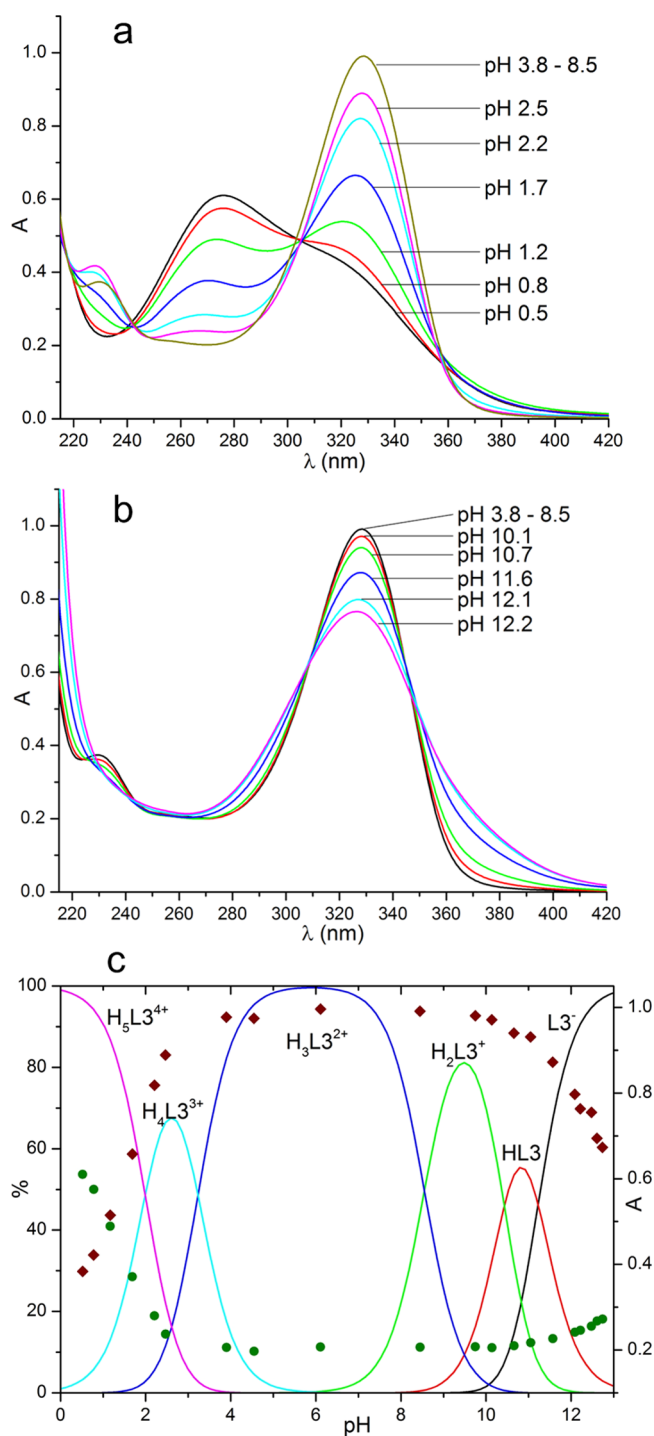


Figure 3. UV absorption spectra of HL3 at different pHs in aqueous solution: (a) pH 0.5–8.5, (b) pH 8.5–12.2, and (c) pH dependence of the 330 nm (red diamonds) and 265 nm (green dots) absorbances.

forms the same species of HL1 with the exclusion of the tetraprotonated one. Such differences are justified by the different numbers of donor atoms in the ligands and, in the case of Cu(II), by the greater stability of the complexes with HL3. Indeed, HL1 and HL3, which can provide at most five donor atoms, are not able to fulfill the coordination sphere of the metal ions, and deprotonation of a coordinated water molecule gives rise to MLOH complexes in alkaline media. On the other hand, HL2, containing one more donor atom, does not form a similar hydroxylate species with Cu(II), whereas the corre-

Table 3. Stability Constants of the Complexes Formed by HL1 and HL2 with Cu^{2+} , Zn^{2+} , and Pd^{2+} in 0.1 M NMe_4Cl at 298.1 ± 0.1 K

equilibria	log K		
	HL1	HL2	HL3
$L^- + Zn^{2+} = [ZnL]^+$	16.3(1) ^a	17.8(1)	19.0(1)
$HL + Zn^{2+} = [ZnHL]^{2+}$	12.62(5)	16.65(6)	13.1(1)
$H_2L^+ + Zn^{2+} = [ZnH_2L]^{3+}$	7.1(1)	11.3(1)	7.8(1)
$[ZnL]^+ + H^+ = [ZnHL]^{2+}$	7.4(1)	10.1(1)	5.3(1)
$[ZnHL]^{2+} + H^+ = [ZnH_2L]^{3+}$	3.8(1)	4.4(1)	5.1(1)
$[ZnL]^+ + OH^- = [ZnLOH]$	4.4(1)	2.8(1)	7.0(2)
$L^- + Cu^{2+} = [CuL]^+$	22.59(6)	21.2(1)	26.0(3)
$HL + Cu^{2+} = [CuHL]^{2+}$	15.65(5)	20.21(9)	18.6(3)
$H_2L^+ + Cu^{2+} = [CuH_2L]^{3+}$		14.74(7)	
$H_4L^{3+} + Cu^{2+} = [CuH_4L]^{5+}$	3.6(2)		
$[CuL]^+ + H^+ = [CuHL]^{2+}$	4.19(6)	10.2(1)	3.9(5)
$[CuHL]^{2+} + H^+ = [CuH_2L]^{3+}$		4.2(1)	
$H_5L^{4+} + Cu^{2+} = [CuH_5L]^{6+}$		3.7(2)	
$[CuL]^+ + OH^- = [CuLOH]$	4.16(8)		7.2(5)

^aValues in parentheses are standard deviations of the last significant figures.

sponding Zn(II) species is significantly less stable than the hydroxylated complexes formed by HL1 and HL3 (Table 3). The most peculiar feature of these complex systems, however, is the gap of protonation states observed for the Cu(II) systems between $CuHL1^{2+}$ and CuH_4L1^{5+} , in the case of HL1, and between CuH_2L2^{3+} and CuH_5L2^{6+} , for HL2 (Table 3, Figure S2). In CuH_4L1^{5+} and CuH_5L2^{6+} , the metal ion is expected to be bound by the pyrimidine group in a chelating mode similar to that observed in the crystal structure of $[Cu(HL1)](ClO_4)_2$, while the macrocyclic ring, being triprotonated, is not able to bind metal ions. As a matter of fact, these highly protonated complexes are formed in very acidic solutions. When the pH is increased and the macrocycle starts releasing the most acidic proton, Cu(II) migrates from the pyrimidine binding site to the macrocycle, forcing the deprotonation of the remaining ammonium groups. Most likely, such a triple deprotonation process does not occur in a single step but takes place through successive equilibria occurring in a pH range so tight that they are not distinguishable, at least by means of the potentiometric method. This is a case of pH-controlled metal translocation similar to that observed with macrocyclic ligands containing divergent binding sites.¹⁰

The UV spectra of the ligands in the presence of metal ions, recorded at various pH values, are shown in Figure 4 for HL2 with Zn(II) and in Figures S3–S5 for the other systems. A comparison of complex spectra with those of the metal-free ligands shows that the 330 nm absorbance is insensitive to the presence of metal ions, whereas the band at 265 nm, due to the pyridine moiety, is enhanced within the entire pH region in which metal complexation takes place, indicating that the pyridine nitrogen atom is involved in the formation of all complex species (Figures 5 and S6). In the case of Cu(II) complexes (Figures 5b and S6b), however, this enhancement is present even in very acidic solutions because, under such conditions, the formation of CuH_4L1^{5+} and CuH_5L2^{6+} , in which the metal ion is coordinated to the pyrimidine residue, enhances the absorbance due to this chromophoric group also occurring at about 260 nm. The profile of the pH dependence of this band is indicative of metal translocation occurring from

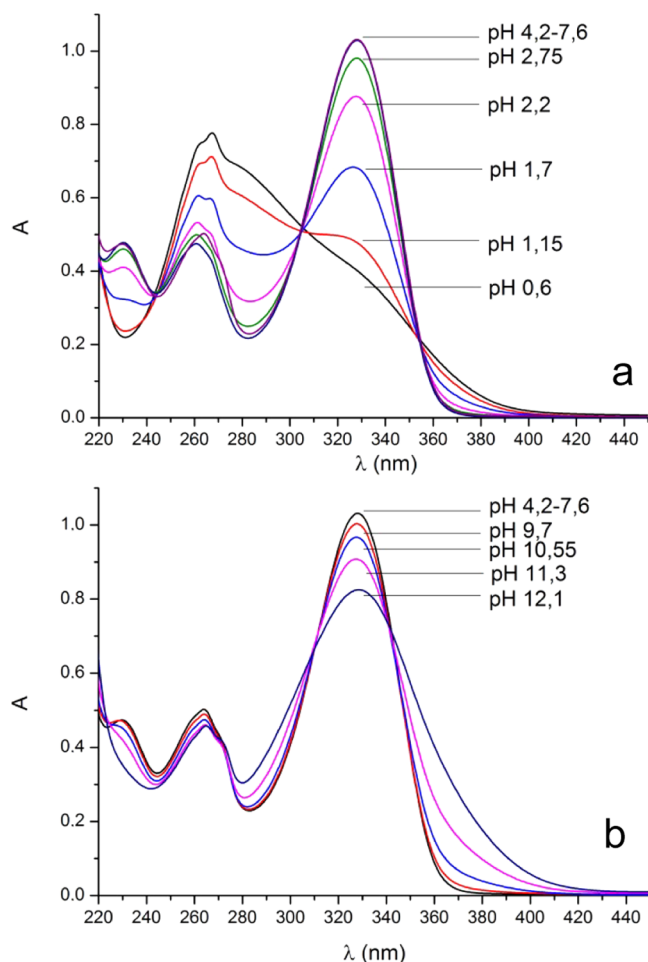


Figure 4. UV spectra of HL2 complexes with Zn²⁺ in the pH ranges 0.6–7.6 (a) and 7.6–12.1 (b). [Zn²⁺] = [HL2] = 5×10^{-5} M. UV spectra for other complex systems are reported in Figures S3 and S4.

pyrimidine to the macrocyclic (pyridine) sites with increasing pH.

As already noted above, for HL3, we did not observe the formation of Cu(II) complexes in a high protonation state, such as CuH₄L1⁵⁺ for HL1, in which the metal ion is chelated by the pyrimidine group. Because of the greater stability of the complexes formed by HL3, a release of the Cu(II) ion from the macrocyclic ring takes place in more acidic solutions (below pH 3), relative to HL1. Accordingly, the hypothetical CuH₄L3⁵⁺ species, is not expected to form in appreciable amounts above pH 2.5, which is the lower pH limit useful for our pH-metric titrations. Nevertheless, we cannot exclude the formation of such species below pH 2.5, although under similar acidic conditions, protonation of the nitroso group becomes an additional impediment.

HL2 binds the two metal ions forming more stable complexes than HL1 and HL3 (Table 3), in agreement with the presence of one more amine group in its lateral chain. In the case of HL1, it is possible to perform a comparison with the coordination properties of the parent ligand 1,^{8c,11} evidencing that the stability of the ZnHL1²⁺ (log K = 12.6) and CuHL1²⁺ (log K = 15.48) complexes is significantly lower than that of the analogous complexes Zn1²⁺ (log K = 17.42)¹¹ and Cu1²⁺ (log K = 20.43, ref 8c), in agreement with the loss of coordinating ability experienced by the primary nitrogen of 1 (Figure 1) upon functionalization with the pyrimidine residue. As a matter

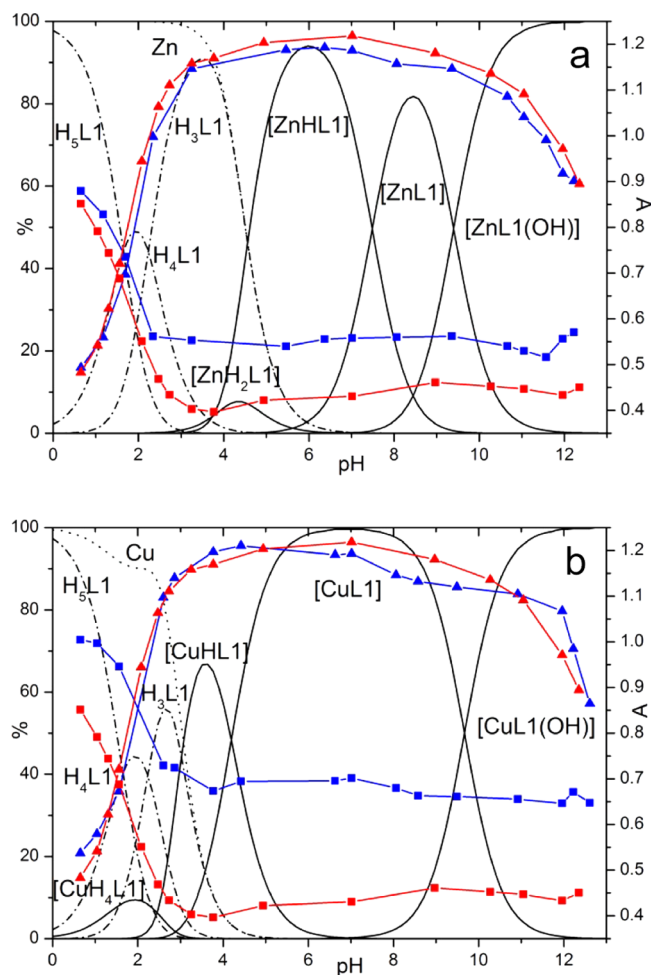


Figure 5. pH dependence of the 330 nm (triangles) and 265 nm (squares) absorbances of HL1 in the absence (red) and presence (blue) of Zn²⁺ (a) and Cu²⁺ (b) superimposed to the relevant species distribution diagrams. [M²⁺] = [L] = 5×10^{-5} M. Species charges have been omitted for simplicity.

of fact, in the crystal structure of CuHL1(ClO₄)₂, this amine group is not involved in the coordination to the metal ion, which completes its coordination environment by chelate binding of the pyrimidine residue of an adjacent complex molecule. Nonetheless, when this functionalized nitrogen undergoes deprotonation, enhancing its coordinating ability, the complex stability increases (Table 3). This phenomenon is much less evident for HL2, as the additional amine group in the lateral chain is already coordinated when the nitrogen atom directly bound to the pyrimidine group becomes deprotonated. The involvement of this deprotonated amine group in metal coordination can be assessed by comparing the equilibrium constants for the protonation of free and complexed ligands according to the general equilibria $L^- + H^+ = HL$ and $ML^+ + H^+ = MHL^{2+}$ ($L = L1, L2, L3$; $M = Zn, Cu$). In the case of HL2, complex protonation constants (log K = 10.42 for ZnL2²⁺, log K = 10.5 for CuL2²⁺, Table 3) are very similar to the protonation constant of L2⁻ (log K = 11.25, Table 2), indicating that the group being protonated is free, whereas in the case of HL1, a similar comparison shows that complex protonation takes place on a coordinated group (log K = 7.4 for ZnL1⁺, log K = 4.02 for CuL1⁺, log K = 5.3 for ZnL3⁺, log K =

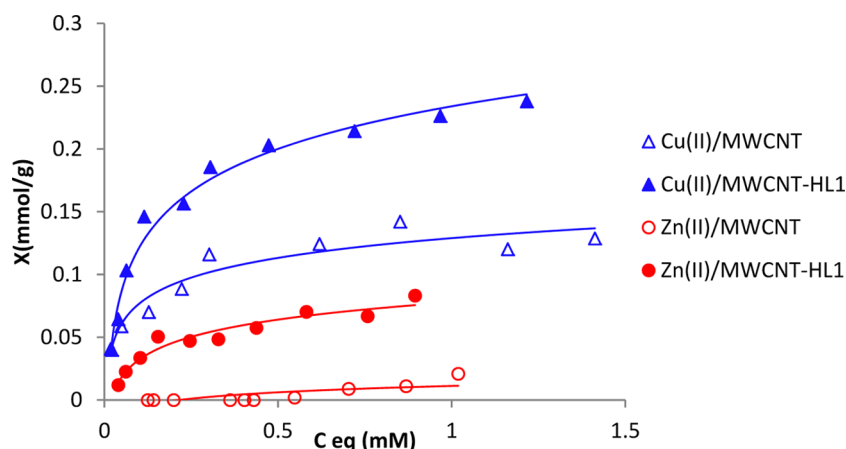


Figure 6. Adsorption isotherms of Cu(II) and Zn(II) on MWCNT and MWCNT-HL1 adsorbents at pH 5.0.

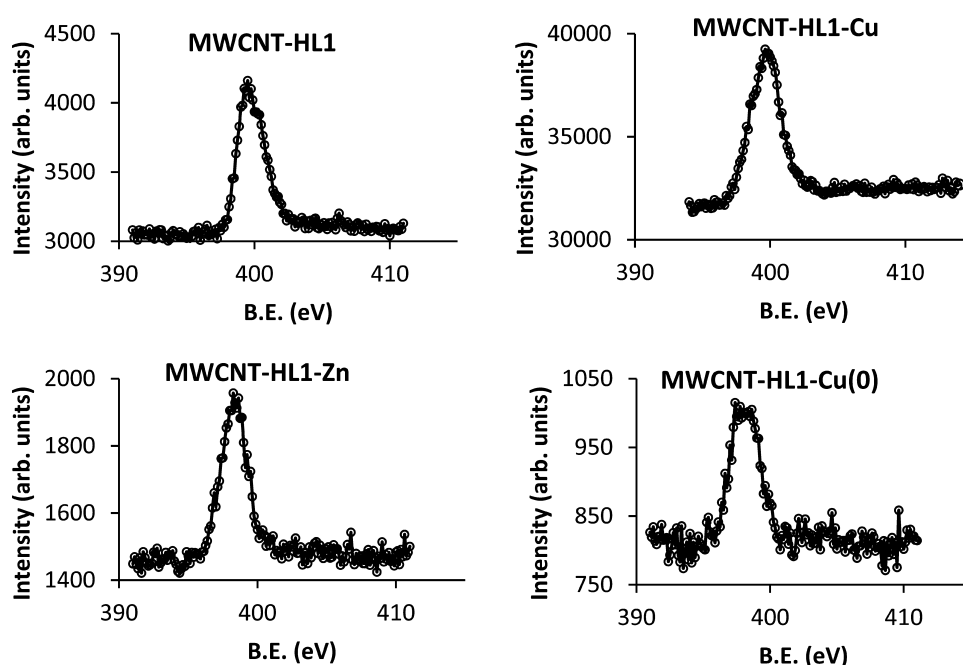


Figure 7. High-resolution XPS spectra in the N1s region.

3.9 for CuL_3^+ vs $\log K = 11.13$ for L_1^- and $\log K = 11.22$ for L_3^-).

Adsorption of Cu(II) and Zn(II) by MWCNT-HL1. To explore the ability of MWCNTs functionalized with these macrocyclic ligands to adsorb metal ions other than the already studied Pd(II), which forms very stable and inert complexes, we checked the MWCNT-HL1/Cu(II) and MWCNT-HL1/Zn(II) systems. According to a reported procedure,¹ hybrid MWCNT-HL1 material, containing 0.36 mmol of HL1 per gram of MWCNT, was prepared by shaking at 298 K a suspension of MWCNT (0.5 g) in an aqueous 10^{-3} M HL1 solution (500 cm^3) at pH 7.5 for 3 days to reach the maximum load of HL1. The MWCNT-HL1 material, resulting after filtration of the equilibrated suspension, water washing, and drying, was employed for the Cu(II) and Zn(II) adsorption tests.

The adsorption isotherms of Cu(II) and Zn(II) ions on MWCNTs and MWCNT-HL1 adsorbents, obtained in water at 298.1 K and pH = 5.0, are shown in Figure 6. The analysis of the equilibrium solutions allowed us to check that HL1 was not

desorbed in the experiments involving MWCNT-HL1. All of the adsorption isotherms were fit to the linear form of the Langmuir eq 1 (except that of the MWCNT/Zn(II) system, see below), where C_e is the adsorbate equilibrium concentration, X is the amount adsorbed, X_m is the maximum adsorption capacity, and K_L is the Langmuir constant.

$$\frac{1}{X} = \frac{1}{K_L X_m C_e} + \frac{1}{X_m} \quad (1)$$

As shown in Figure 6, at pH = 5.0, the pristine MWCNTs bind Cu(II) to a significant extent, with a maximum adsorption capacity, calculated from the above equation, $X_m = 0.13(1)$ mmol/g of adsorbent. In contrast, in the case of Zn(II), the adsorption is insignificant. The results can be explained by considering that the adsorption of a metal ion from aqueous solution onto a graphene surface takes place by interactions of the $\text{C}\pi(\text{a soft base})-\text{d}\pi$ type,¹² which is expected to be stronger for the acidic Cu(II) than for Zn(II).

The Cu(II) and Zn(II) loads increase significantly upon functionalization of the MWCNTs with HL1. In the case of

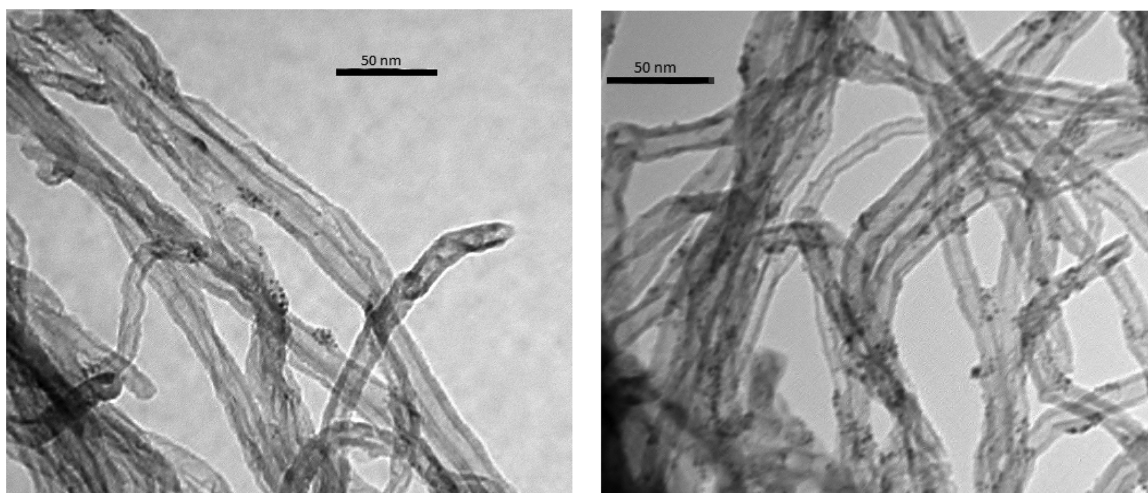


Figure 8. TEM Images of MWCNT-HL1-Cu(0).

Cu(II), the X_m value increases up to 0.24(1) mmol/g, relative to MWCNT-HL1, whereas in the case of Zn(II), it also increases significantly from ca. 0 to 0.080(4) mmol/g (Figure 6). In a previous work,¹ the characterization of MWCNT-HL1 showed that π - π stacking interaction of the pyrimidine moiety of the adsorbed HL1 with the $C\pi$ centers of MWCNT results in the loss of (Brønsted) basicity by the pyrimidine conjugate C(5)-NO group, whereas the basicity of the polyamine function is preserved to a good extent, allowing the adsorption, via complexation, of Pd(II) ions by MWCNT-HL1.¹ Accordingly, also the adsorptivity enhancement observed for MWCNT-HL1 with Cu(II) and Zn(II), relative to pristine MWCNT, is expected to occur via metal coordination to the macrocyclic moiety of HL1. Indeed, like in the case of Pd(II), upon adsorption of Cu(II) by MWCNT-HL1, the aliphatic component of the X-ray photoelectron spectroscopy (XPS) N1s signal corresponding to the polyamine moiety (Figure 7) shifts to higher binding energy (BE) values, compared to those of the metal-free MWCNT-HL1, in agreement with the high strength of the Cu(II)-polyamine interaction (Table 3). On the contrary, in the case of MWCNT-HL1-Zn(II), the N1s component of the XPS spectrum shifts to lower BE values. The latter effect, which is the opposite to that observed with Cu(II) and Pd(II),¹ can be ascribed to the fact that the binding of Zn(II) to HL1 polyamine nitrogen atoms in MWCNT-HL1-Zn is weaker than the binding of protons by MWCNT-HL1 at the working pH (5). In fact, the equilibrium data for the HL1-Zn(II) system (Table 3 and Figure 5) show that, at pH = 5, ligand protonation competes efficiently with Zn(II) coordination.

The presence, in the Cu2p range of the XPS spectrum of MWCNT-HL1-Cu(II), of a single peak at 933.6 eV with a satellite at 944.0 eV (corresponding to the release of Cu2p_{3/2} electrons) and of another peak at 953.9 eV (assigned to Cu2p_{1/2} electrons), typical of Cu(II),¹³ discards any metal reduction during the adsorption process and suggests that all copper is adsorbed as Cu(II) coordinated to the polyamine (Supporting Information). In the case of MWCNT-HL1-Zn(II), the presence of Zn(II) is confirmed by a well-defined XPS signal at 1020.1 eV corresponding to the release of Zn²p_{3/2} electrons (Supporting Information).

According to the equilibrium data (Table 3) for the formation of HL1 complexes with Cu(II), the ligand environ-

ment of the coordinated Cu(II) in MWCNT-HL1-Cu(II) should be formed by four polyamine nitrogen atoms, which leave space for the additional coordination of water molecules or/and hydroxyl groups. The presence of hydroxyl ligands coordinated to Cu(II) in MWCNT-HL1-Cu(II) is suggested by the quantitative analysis of its XPS spectrum, which provides an atomic relationship, Cu/Cl \approx 2/1. As charge neutrality requires two negative charges for each Cu(II) in the sample, it seems likely that the missing Cl⁻ ions were replaced by OH⁻ groups upon the repeated washing of MWCNT-HL1-Cu(II) performed in the final stage of its preparation (see Experimental Section). A similar conclusion is reached in the case of MWCNT-HL1-Zn(II), for which the Zn/Cl atomic relationship obtained from its XPS spectrum is also \approx 2/1. Thus, Zn(II) adsorbed in this material should be complexed by the ligand polyamine moiety (although more weakly coordinated than in the case of Cu(II)) and by additional water molecules and/or hydroxyl groups.

Metal-ion adsorption by a polyamine-complexation mechanism explains that the X_m values of MWCNT-HL1 with Zn(II) and Cu(II) at pH = 5.0 follow the same trend of the corresponding effective stability constants (K_{eff})¹⁴ at this pH (log K_{eff} = 4.48 for Zn(II) and log K_{eff} = 9.33 for Cu(II)). In the case of other metal ions, such as Pd(II), which is expected to form more stable complexes with HL1¹ than Zn(II) and Cu(II), the adsorption capacity of MWCNT-HL1 is also much higher.¹

In previous works,^{1,15} we studied the behavior of Pd catalysts based on Pd(0) nanoparticles and Pd(II) supported on: (i) an activated carbon functionalized with a tren-derivative ligand and (ii) the MWCNT-HL1 and MWCNT-HL2 materials used in this work. In these studies, it was found that the catalytic efficiency and the robustness of the catalysts increase with the binding ability of surface functions.^{1,15} On this background and on account of the implication of Cu-based nanoparticles as catalysts in a wide range of reactions,⁴ we found it interesting to test the possibility of obtaining functionalized MWCNTs with surface-stabilized Cu(0) nanoparticles using our hybrid materials. To this purpose, a MWCNT-HL1-Cu(II) sample was treated with NaBH₄ by following the procedure described in Experimental Section. The XPS of this sample showed the lack of Cu(II) peaks and the appearance of two peaks at 951.0 and 930.1 eV corresponding to Cu(0)2p_{1/2} and Cu(0)2p_{3/2},¹³

indicating a quantitative reduction of Cu(II) to Cu(0) (Supporting Information). This reduction is also accompanied by a loss of oxygen from 2.75 to 2.15 atom %, which can be ascribed to the removal of water and hydroxyl ligands. It is very significant that the nitrogen content after reduction remains unchanged (3.09 and 3.04 atom % for unreduced and reduced MWCNT-HL1-Cu, respectively) as also occurs for the Cu one (0.35 and 0.34 atom % for unreduced and reduced MWCNT-HL1-Cu, respectively). This shows that, despite the relatively drastic conditions used for the reduction, neither HL1 nor Cu lixiviate during sample reduction and successive repeated washing, pointing out a significant stability of the material. This is not surprising, according to the proven stability of the π - π interactions in similar systems.² Concerning the Cu(0) nanoparticles, their interactions with the MWCNT surface, illustrated by the transmission electron microscopy (TEM) images in Figure 8, are reinforced by interaction with the polyamine residue of HL1 molecules protruding from the surface. As a matter of fact, shifting of the XPS N1s signal to a significantly lower BE, relative to MWCNT-HL1, suggests that the unprotonated polyamine residues of MWCNT-HL1-Cu(0) interact with the surface Cu(0) nanoparticles.¹⁵ It is noteworthy that the result obtained by XPS analysis for the Cu(0) content of the reduced sample is equal to the Cu(II) content of the parent MWCNT-HL1-Cu(II), meaning that such Cu(0) nanoparticles should be very small. Actually, because of the low penetrating power of the radiation used in the XPS analysis, an accurate quantitative determination of metal from nanoparticles, by this technique, is only possible for very small nanoparticles (the bigger the nanoparticle, the lower the amount of metal detected compared to the real one). Indeed, the detected nanoparticles are smaller than 5 nm. This is illustrated in Figure 8, which also shows the uniformity of their size and distribution on the external surface of the MWCNTs.

The whole results obtained in this section show that the structural characteristics and the stability of both MWCNT-HL1-Cu(II) and MWCNT-HL1-Cu(0) make them promising Cu-based materials to be assayed as potentially active and robust solid catalysts.

CONCLUSIONS

In summary, the results of this work show that metal-ion adsorption by materials of the MWCNT-HL1 type represents a suitable procedure for the preparation of heterogeneous catalysts based on HL1-metal complexes adsorbed on the MWCNT surface. The preparation procedure, which is characterized by very mild, environmentally friendly conditions, provides an efficient control for MWCNT surface functionalization, which is a crucial factor for an efficient transfer of the catalytic properties of the HL1-metal complex to the MWCNT surface.

The adsorption results show how the reactivity of the polyamine function of HL1 toward Zn(II) and Cu(II) determines the preferential adsorption of these ions on MWCNT-HL1 via coordination to HL1. This determines a higher adsorption capacity for Cu(II) than for Zn(II) and gives rise to hybrid materials consisting of MWCNTs containing HL1-Cu(II) and HL1-Zn(II) complexes homogeneously distributed on the external graphene surface of the MWCNTs. In view of our previous results, showing high catalytic efficiency of an analogous Pd(II) derivative, and taking into account the high thermodynamic stability of the Cu(II) complex, we expect that MWCNT-HL1-Cu(II) might behave as a robust and

reusable catalyst for reactions in which Cu(II)-based catalysts have proven their efficiency.⁴ Moreover, reduction of MWCNT-HL1-Cu(II) provides a Cu(0)-nanostructured MWCNT hybrid material, whose structure and stability are very promising for its application in reactions requiring Cu(0)-based catalysts. This will be the focus of further research work.

EXPERIMENTAL SECTION

Materials. Unless otherwise specified, all starting materials were purchased from commercial sources and used as supplied. Thin MWCNTs with metal oxide content $\leq 5\%$ were purchased from Nanocyl (Ref 3100). HL1 and HL2 were obtained according to a previously reported synthetic procedure.¹ The MWCNT-HL1 hybrid material was prepared as previously reported.¹

Synthesis of HL3. HL3 was prepared by the reaction of 1,4,8,11-tetraazacyclotetradecane-1-ethanamine¹⁶ (3 in Figure 1) with 6-amino-3,4-dihydro-3-methyl-2-methoxy-5-nitroso-4-oxopyrimidine according to the procedure previously described¹ for the synthesis of HL1 and HL2. Yield 95%. $C_{18.5}H_{31}N_9O_{3.5}$ (HL3-0.5MeOH·H₂O): calcd C 51.02, H 7.18, N 28.94; found C 50.93, H 7.19, N 28.70. ¹H NMR D₂O: δ (ppm) 2.62–3.46 (m, 13H), 3.74 (t, 2H), 4.55 (s, 4H), 7.37 (d, 2H), 7.88 (t, 1H).

Synthesis of [Cu(HL1)](ClO₄)₂. Crystals of the complex suitable for X-ray analysis were obtained by slow evaporation at room temperature of an ethanolic solution containing HL1 and Cu(ClO₄)₂·6H₂O in equimolar amounts. **Caution!** Perchlorate salts of metal complexes are potentially explosive. Only a small amount of material should be prepared and handled with care.

Potentiometric Measurements. Potentiometric (pH-metric) titrations, used to determine ligand protonation and complex stability constants, were performed in 0.1 M NMe₄Cl at 298.1 \pm 0.1 K using an automated apparatus and a procedure previously described.¹⁷ The combined Metrohm 6.0262.100 electrode was calibrated as a hydrogen-ion concentration probe by titrating previously standardized amounts of HCl with CO₂-free NaOH solutions and determining the equivalent point by Gran's method,¹⁸ which gives the standard potential, E° , and the ionic product of water ($pK_w = 13.83(1)$ in 0.1 M NMe₄Cl at 298.1 K). Computer program HYPERQUAD¹⁹ was used to calculate ligand protonation and complex stability constants from potentiometric data. The concentration of the ligands was about 1×10^{-3} M, whereas the concentration of metal ions (M) was $[M] \approx 0.8[L]$. The studied pH range was 2.5–11.5, unless otherwise noted. Both complex formation and dissociation reactions of HL3 with Zn(II) and Cu(II), occurring during the potentiometric titrations, appeared to be very slow, although the dissociation processes were much faster than the formation ones. For this reason, these systems were studied following complex dissociation, that is, by performing the potentiometric titrations from alkaline to acidic conditions. In the case of Zn(II), the alkaline solution of the complex was prepared in the potentiometric cell and the pH variation was monitored until equilibrium was reached (2 h). Then, the solution was titrated with a standardized HCl solution. A duration of 45 min was necessary to reach the equilibrium after each addition. In the case of Cu(II), 2 days were necessary to reach the equilibrium of the starting solution. Accordingly, the alkaline complex solution was prepared in a separate vessel, stored in an inert atmosphere, left to equilibrate for 2 days at 298 K, and then transferred into the titration cell. The measurement was performed as in the case of Zn(II) but with

an elapsed time of 2 h between successive titrant (acid) additions. In the case of Cu(II), the pH range investigated was 2.5–8. At least two measurements were performed for each system, both for ligand protonation and for metal-ion-complexation experiments. For all systems, the different titration curves were treated as separated curves without significant variations in the values of the calculated stability constants. Finally, the sets of data were merged and treated simultaneously to give the final stability constants. Different equilibrium models for the complex systems were generated by eliminating and introducing different species. Only those models for which the HYPERQUAD program furnished a variance of the residuals $\sigma^2 \leq 9$ were considered acceptable. Such a condition was unambiguously met by a single model for each system.

Spectrophotometric Measurements. Absorption spectra were recorded at 298 K on a Jasco V-670 spectrophotometer. The concentrations of both ligand and metal complex solutions were about 5×10^{-5} M. ^1H NMR spectra (400 MHz) in D_2O solution were recorded at 298 K on a 400 MHz Bruker Avance III spectrometer.

Crystallography. Crystallographic data for $\text{CuHL1}(\text{ClO}_4)_2$: $\text{C}_{18}\text{H}_{27}\text{Cl}_{12}\text{CuN}_9\text{O}_{10}$, MW = 663.94, orthorhombic, *Pbca*, $a = 14.2264(4)$ Å, $b = 18.2109(5)$ Å, $c = 18.9638(5)$ Å, $V = 4913.1(2)$ Å³, $Z = 8$, $\rho_{\text{calcd}} = 1.795$ g cm⁻³, μ (Cu K α) = 3.938 mm⁻¹, $T = 150$ K, $R_1 = 0.0595$ (for 2479 reflections with $I > 2s(I)$), $wR_2 = 0.1010$ (all data), and GOF = 1.025. The crystals gave poor diffraction, so the resolution was limited to theta max = 62°. Data collection was carried out using an Oxford Diffraction XcaliburPX instrument equipped with a copper anode ($\lambda = 1.5418$ Å). A summary of the crystallographic data is reported in Table S2. The integrated intensities were corrected for Lorentz and polarization effects and absorption correction was applied.²⁰ The structure was solved by direct methods (SIR92).²¹ Refinement was performed by means of full-matrix least-squares using SHELXL-2014/7 program.²² All nonhydrogen atoms were anisotropically refined. Hydrogen atoms were introduced in calculated positions, and their coordinates and isotropic displacement factors were refined in agreement with the linked carbon atoms.

Crystallographic data have been deposited with the Cambridge Crystallographic Data Center (CCDC 1553257).

Adsorption Measurements. Adsorption isotherms of Cu(II) and Zn(II) ions on MWCNTs and MWCNT-HL1 adsorbents were carried out at 298.1 K, according to the experimental procedure previously reported.²³ Under typical conditions, 0.050 g of each adsorbent were placed in contact with 25 mL of an aqueous solution of the corresponding metal dichloride at pH 5.0. The samples were shaken in a thermostated air incubator until equilibrium was reached (5 days). The adsorbate concentration ranged from 1×10^{-4} to 1.7×10^{-3} M. The concentration of the ions was determined by atomic absorption spectrometry using a PerkinElmer Analyst 800 equipment. The analysis of the equilibrium solutions allowed us to check that HL1 was not desorbed when the MWCNT-HL1 hybrid material was used as adsorbent.

Preparation of MWCNT-HL1-Cu(0). A sample (43.9 mg) of MWCNT-HL1-Cu (containing 0.157 mmol of Cu(II) per gram of MWCNT-HL1), which was obtained from the adsorption isotherm experiment (see above), was mixed with 10 mL of water, and the mixture was added to 22 mg of NaBH_4 , (molar Cu(II)/ $\text{NaBH}_4 = 1/80$). The mixture was left to react under stirring for 2 h at room temperature. After this,

the resulting solid was separated by filtration, washed repeatedly with doubly distilled water, and dried in a desiccator under silica until a constant weight was obtained.

XPS Spectra. The XPS spectra of solid samples MWCNT-HL1-Cu, MWCNT-HL1-Cu(0), and MWCNT-HL1-Zn were recorded with a ESCA5701 instrument (Physical Electronics), using the Mg K α 300 W, 15 kV radiation of the twin anode in the constant analyzer energy mode, with pass energies of 187.85 and 29.35 eV for the survey and high-resolution spectra, respectively. The pressure of the analysis chamber was maintained at 10^{-9} T, and the BE and the Auger kinetic energy scale were regulated by setting the C1s transition at 284.6 eV. The accuracy of BE values was 0.2 eV.

TEM Micrographs. TEM images of the MWCNT-HL1-Cu(0) sample have been obtained with a JEOL Mod. JEM-1010 equipment.

■ ASSOCIATED CONTENT

■ Supporting Information

The Supporting Information is available free of charge on the ACS Publications website at DOI: 10.1021/acsomega.7b00736.

Crystal and structure refinement data; geometric parameters for the anion- π contact; distribution diagrams for HL3 protonation and Cu(II) and Zn(II) complexation with HL1–HL3; UV spectra at variable pH values of Cu(II) and Zn(II) complexes with HL1 and HL2 and of Cu(II) complexes with HL3; high-resolution XPS spectra of MWCNT-HL1-Cu(II), MWCNT-HL1-Cu(0), and MWCNT-HL1-Zn(II) (PDF)

■ AUTHOR INFORMATION

Corresponding Authors

*E-mail: antonio.bianchi@unifi.it (A.B.).

*E-mail: enrique.garcia-es@uv.es (E.G.E.).

*E-mail: rlopez@ujaen.es (R.L.G.).

ORCID

Antonio Bianchi: 0000-0002-1082-3911

Notes

The authors declare no competing financial interest.

■ ACKNOWLEDGMENTS

Support from Italian MIUR (Project 2015MP34H3), MINECO (Project MAT2014-60104-C2-2-R), Autonomous Regional Government (Junta de Andalucía, Group PAIDI FQM273), University of Jaén (EI-FQM6_2017), Spanish Ministerio de Economía y Competitividad (projects CTQ2013-48917-C3-1-P, CTQ2016-78499-C6-1-R, and Unidad de Excelencia MDM 2015-0038), and Generalitat Valenciana (Project PROMETEOII2015-002) is gratefully acknowledged.

■ REFERENCES

- (1) Savastano, M.; Arranz-Mascarós, P.; Bazzicalupi, C.; Clares, M. P.; Godino-Salido, M. L.; Gutiérrez-Valero, M. D.; Inclán, M.; Bianchi, A.; García-España, E.; López-Garzón, R. Construction of Green Nanostructured Heterogeneous Catalysts via Non-Covalent Surface Decoration of Multi-Walled Carbon Nanotubes with Pd(II) Complexes of Azamacrocycles. *J. Catal.* **2017**, 000, 000.
- (2) López-Garzón, R.; Godino-Salido, M. L.; Gutiérrez-Valero, M. D.; Arranz-Mascarós, P.; Melguizo, M.; García, C.; Domingo-García, M.; López-Garzón, F. J. Supramolecular assembling of molecular ion-ligands on graphite-based solid materials directed to specific binding of metal ions. *Inorg. Chim. Acta* **2014**, 417, 208–221.

- (3) Bazzicalupi, C.; Bianchi, A.; García-España, E.; Delgado-Pinar, E. Metals in supramolecular chemistry. *Inorg. Chim. Acta* **2014**, *417*, 3–26.
- (4) Gawande, M. B.; Goswami, A.; Felpin, F. X.; Asefa, T.; Huang, X.; Silva, R.; Zou, X.; Zboril, R.; Varma, R. S. Cu and Cu-Based Nanoparticles: Synthesis and Applications in Catalysis. *Chem. Rev.* **2016**, *116*, 3722–3811.
- (5) (a) Nakatake, D.; Yokote, Y.; Matsushima, Y.; Yazakia, R.; Ohshima, T. A highly stable but highly reactive zinc catalyst for transesterification supported by a bis(imidazole) ligand. *Green Chem.* **2016**, *18*, 1524–1530. (b) Bencini, A.; Berni, E.; Bianchi, A.; Fedi, V.; Giorgi, C.; Paoletti, P.; Valtancoli, B. Carboxy and diphosphate ester hydrolysis promoted by dinuclear zinc(II) macrocyclic complexes. Role of Zn(II)-bound hydroxide as the nucleophilic function. *Inorg. Chem.* **1999**, *38*, 6323–6325. (c) Bazzicalupi, C.; Bencini, A.; Berni, E.; Bianchi, A.; Fornasari, P.; Giorgi, C.; Valtancoli, B. Zn(II) coordination to polyamine macrocycles containing dipyrindine units. New insights into the activity of dinuclear Zn(II) complexes in phosphate ester hydrolysis. *Inorg. Chem.* **2004**, *43*, 6255–6265.
- (6) Comerford, J. W.; Hart, S. J.; North, M.; Whitwood, A. C. Homogeneous and silica-supported zinc complexes for the synthesis of propylene carbonate from propane-1,2-diol and carbon dioxide. *Catal. Sci. Technol.* **2016**, *6*, 4824–4831.
- (7) Bianchi, A.; Micheloni, M.; Paoletti, P. Thermodynamic aspects of the polyazacycloalkane complexes with cations and anions. *Coord. Chem. Rev.* **1991**, *110*, 17–113.
- (8) (a) Clares, M. P.; Serena, C.; Blasco, S.; Nebot, A.; Del Castillo, L.; Soriano, C.; Domènech, A.; Sánchez-Sánchez, A. V.; Soler-Calero, L.; Mullor, J. L.; García-España, A.; García-España, E. Mn(II) complexes of scorpion-like ligands. A model for the MnSOD active centre with high in vitro and in vivo activity. *J. Inorg. Biochem.* **2015**, *143*, 1–8. (b) Blasco, S.; Verdejo, B.; Clares, M. P.; Castillo, C. E.; Algarra, A. G.; Latorre, J.; Máñez, M. A.; Basallote, M. G.; Soriano, C.; García-España, E. Hydrogen and Copper Ion Induced Molecular Reorganizations in Two New Scorpion-Like Ligands Appended with Pyridine Rings. *Inorg. Chem.* **2010**, *49*, 7016–7027. (c) Verdejo, B.; Ferrer, A.; Blasco, S.; Castillo, C. E.; González, J.; Latorre, J.; Máñez, M. A.; García Basallote, M.; Soriano, C.; García-España, E. Hydrogen and Copper Ion-Induced Molecular Reorganizations in Scorpion-like Ligands. A Potentiometric, Mechanistic, and Solid-State Study. *Inorg. Chem.* **2007**, *46*, 5707–5719. (d) Inclán, M.; Albelda, M. T.; Frías, J. C.; Blasco, S.; Verdejo, B.; Serena, C.; Salat-Canela, C.; Díaz, M. L.; García-España, A.; García-España, E. Modulation of DNA Binding by Reversible Metal-Controlled Molecular Reorganizations of Scorpion-like Ligands. *J. Am. Chem. Soc.* **2012**, *134*, 9644–9656.
- (9) (a) Savastano, M.; Arranz-Mascarós, P.; Bazzicalupi, C.; Bianchi, A.; Giorgi, C.; Godino-Salido, M. L.; Gutiérrez-Valero, M. D.; López-Garzón, R. Binding and removal of octahedral, tetrahedral, square planar and linear anions in water by means of activated carbon functionalized with a pyrimidine-based anion receptor. *RSC Adv.* **2014**, *4*, 58505–58513. (b) Arranz, P.; Bianchi, A.; Cuesta, R.; Giorgi, C.; Godino, M. L.; Gutiérrez, M. D.; López, R.; Santiago, A. Binding and Removal of Sulfate, Phosphate, Arsenate, Tetrachloromercurate, and Chromate in Aqueous Solution by Means of an Activated Carbon Functionalized with a Pyrimidine-Based Anion Receptor (HL). Crystal Structures of $[\text{H}_3\text{L}(\text{HgCl}_4)] \cdot \text{H}_2\text{O}$ and $[\text{H}_3\text{L}(\text{HgBr}_4)] \cdot \text{H}_2\text{O}$ Showing Anion- π Interactions. *Inorg. Chem.* **2010**, *49*, 9321–9332.
- (10) Anda, C.; Bazzicalupi, C.; Bencini, A.; Bianchi, A.; Fornasari, P.; Giorgi, C.; Valtancoli, B.; Lodeiro, C.; Parola, A. J.; Pina, F. Cu(II) and Ni(II) complexes with dipyrindine-containing macrocyclic polyamines with different binding units. *Dalton Trans.* **2003**, 1299–1307. Bencini, A.; Bianchi, A.; Danesi, A.; Giorgi, C.; Mariani, P.; Valtancoli, B. pH-Controlled metal translocation outside/inside the cavity of a polyamine macrocycle. *J. Coord. Chem.* **2009**, *62*, 82–91.
- (11) González, J.; Llinares, J. M.; Belda, R.; Pitarch, J.; Soriano, C.; Tejero, R.; Verdejo, B.; García-España, E. Tritopic phenanthroline and pyridine tail-tied aza-scorpionands. *Org. Biomol. Chem.* **2010**, *8*, 2367–2376.
- (12) Biniak, S.; Pakula, M.; Szymansky, G. S.; Swiatkowski, A. Effect of Activated Carbon Surface Oxygen- and/or Nitrogen-Containing Groups on Adsorption of Copper(II) Ions from Aqueous Solution. *Langmuir* **1999**, *15*, 6117–6122.
- (13) NIST data base. https://srdata.nist.gov/xps/main_search_menu.aspx.
- (14) (a) Bazzicalupi, C.; Bianchi, A.; Giorgi, C.; Clares, M. P.; García-España, E. Addressing selectivity criteria in binding equilibria. *Coord. Chem. Rev.* **2012**, *256*, 13–27. (b) Bianchi, A.; García-España, E. The use of calculated species distribution diagrams to analyze thermodynamic selectivity. *J. Chem. Educ.* **1999**, *76*, 1727–1732.
- (15) Godino-Salido, M. L.; Gutiérrez-Valero, M. D.; López-Garzón, R.; Arranz-Mascarós, P.; Santiago-Medina, A.; Melguizo, M.; Domingo-García, M.; López-Garzón, F. J.; Abdelkader-Fernández, V. K.; Salinas-Martínez de Lecea, C.; Román-Martínez, M. C. New hybrid materials based on the grafting of Pd(II)-amino complexes on the graphitic surface of AC: preparation, structures and catalytic properties. *RSC Adv.* **2016**, *6*, 58247–58259.
- (16) Pallavicini, P. S.; Perotti, A.; Poggi, A.; Seghi, B.; Fabbrizzi, L. N-(aminoethyl)cyclam: a tetraaza macrocycle with a coordinating tail (scorpionand). Acidity controlled coordination of the side chain to nickel(II) and nickel(III) cations. *J. Am. Chem. Soc.* **1987**, *109*, 5139–5144.
- (17) Bazzicalupi, C.; Bianchi, A.; Biver, T.; Giorgi, C.; Santarelli, S.; Savastano, M. Formation of Double-Strand Dimetallic Helicates with a Terpyridine-Based Macrocycle. *Inorg. Chem.* **2014**, *53*, 12215–12224.
- (18) Gran, G. Determination of the equivalence point in potentiometric titrations. Part II. *Analyst* **1952**, *77*, 661–671.
- (19) Gans, P.; Sabatini, A.; Vacca, A. Investigation of equilibria in solution. Determination of equilibrium constants with the HYPERQUAD suite of programs. *Talanta* **1996**, *43*, 1739–1753.
- (20) CrysAlisPro, version 1.171.35.11; Agilent Technologies, 2015.
- (21) Altomare, A.; Cascarano, G.; Giacovazzo, C.; Guagliardi, A.; Burla, M. C.; Polidori, G.; Camalli, M. SIRPOW.92 – a program for automatic solution of crystal structures by direct methods optimized for powder data. *J. Appl. Crystallogr.* **1994**, *27*, 435–436.
- (22) Sheldrick, G. M. Crystal structure refinement with SHELXL. *Acta Crystallogr., Sect. C: Struct. Chem.* **2015**, *71*, 3–8.
- (23) Godino-Salido, M. L.; Santiago-Medina, A.; Arranz-Mascarós, P.; López-Garzón, R.; Gutiérrez-Valero, M. D.; Melguizo, M.; López-Garzón, F. J. Novel active carbon/crown ether derivative hybrid material for the selective removal of Cu(II) ions: the crucial role of the surface chemical functions. *Chem. Eng. Sci.* **2014**, *114*, 94–104.